Chapter 4

Phonon Properties of III-V Nitrides under Pressure

4.1 Introduction

The search for new semiconductors with improved electronic properties resulted into discovery of binary and multinary compound semiconductors. The interest in the binary semiconductors belonging to II-VI (e.g. ZnSe, CdTe etc.) and III-V (e.g. GaAS, GaSb, AlN etc.) has led to it's foundation since last four decades or so. This has largely motivated due to the desire to fabricate new, efficient, and economic semiconductor devices. As one proceeds from well known group IV (e.g. Si, Ge) elements to the II-VI and III-V compound semiconductors, new properties of such materials are discovered for their understanding and exploration. The availability of large energy band gap and high mobility of electrons in compound semiconductors has led to several useful devices such as hetrojunction lasers, LED, magnetoresistance devices etc. This choice has been still widened with the development of nanostructures in which there occurs lowering in crystal symmetry and dimension thereby leading to devices with interesting properties. Also, in the recent past there have been increasing interest and undesirable experimental and theoretical activities focused on a new group of semiconductors [1-8] which have some unique properties that enhance their potential use in a wide range of opto electronic device applications. Due to these interesting features they have both defense and commercial application. Worldwide experimental and theoretical efforts have been directed towards understanding the underlying physics of the special features associated with these semiconductors. The importance of these materials was recognized when Kamarove [7] first reported the giant enhancement of magneto optical effects in Mn doped II-VI semiconductor CdTe i.e $Cd_{1-x}Mn_xTe$. The materials are known as dilute magnetic semiconductors (DMS) or semi-magnetic semiconductors (SMSC). Nowadays due to the tunability of their energy gap in a wide range, these materials are excellent

candidates for the preparation of quantum wells and superlattices. The semi-magnetic properties bring new physical effects into the already rich, existing spectrum of phenomenon of quantum well, and superlattices. The DMS will be discussed at the length in the chapter 6.

In the recent years, III-V nitrides have gained a status of highly attractive materials because of their great potential in short wave length optoelectronic devices [9]. The nitrides have made possible to have three primary color semiconductor diodes, which have a great impact on imaging and graphics applications. Like most other wide band gap semiconductors, the nitrides exhibit superior radiation hardness compared with GaAs and Si, which also make them attractive for space applications. Although nitrides are well known to be highly stable in the wurtzite structure, zinc blende nitrides has been experimentally observed [10]. It is expected that zinc blende nitrides are more amenable to doping than wurtzite nitrides, since all of the III-V semiconductors that can be efficiently doped are cubic. Therefore, it is meaningful to characterize both experimentally and theoretically the physical properties of zinc blende III-V nitrides. Even though, there is a remarkable progress in the fabrication technology and growth of nitrides, particularly GaN and AlN, some basic properties of these materials remained poorly studied. The phonon spectrum is one of the fundamental characteristics of the crystals. The behavior of the phonon dispersion branches reflects specific features of the crystal structure and the interatomic interactions and therefore gives the most comprehensive and detailed information about dynamical properties of crystals. The phonon dispersion curves are typically obtained by neutron scattering techniques. However, the absence of III-V nitrides crystals of sufficiently large size makes neutron scattering difficult. Other than nitrides the lattice vibrational properties of III-V compound semiconductors have been studied extensively in the last few decades both theoretically and experimentally [8,11-23] that play an important role in the interpretation of electrical resistivity and other transport phenomenon leading to the applications of these semiconducting compounds. The availability of neutron scattering data on phonon in the zinc blende structure semiconductors has made it possible to make theoretical studies of crystal properties and also ultimately has led to the development of number of

theoretical models to interpret them. Out of several models, rigid ion model (RIM) [25], shell model (SM) [26], valance force field model (VFFM) [27] deformation dipole model and deformation bond approximation model (DDM and DBA) [28] have been quite successful in interpreting the experimental observations.

Like other solids, semiconductors in general and group III-V compounds in particular are also forced to exhibit a number of structural transition under hydrostatic pressure [29]. Depending on the system, the transition pressure range from several tens of K bars to few hundred K bars. Raman scattering investigations have revealed valuable information regarding the changes in the phonon spectrum across the phase transition [30] and in identifying soft phonon modes believed to be responsible for driving the phase transition [31]. As far as the pressure dependent experimental or theoretical investigation on the phonon properties are concerned there are few reports by using Raman spectroscopy [31,32-35] and theoretical methods [36-38] limited to compound semiconductors other than nitrides. K. Karch [39] and C. Gobel [40] have reported first principle calculation of the structural, lattice dynamical and dielectric properties for zinc blende and wurtzite AlN. While most of the studies are performed for the wurtzite and hexagonal structure, the situation is poor for III-V nitrides in its ZB structure. Miwa and Fukumoto [41] and Kim [42] have calculated the frequency of TO phonon mode at zone center using first principle method. Rare attempts of high pressure study of these compounds have been reported so far. Perlin [43] has reported structural properties with x-ray absorption spectroscopy and vibrational properties with Raman scattering. These facts motivated us to investigate phonon properties of III-V nitrides through out the Brillouin zone at ambient and high pressure. In the present chapter we report the results of our investigations on pressure dependent phonon dispersion curves, phonon density of states, mode Grüneisen parameters and specific heat for four III-V nitrides namely AlN, GaN, BN and InN by using rigid ion model already discussed in previous chapter. In addition we have also reported variation in the phonon frequencies at different points in the BZ with pressure for mentioned phosphides. We have also performed study of variation of LO-TO splitting at Γ point with pressure. In section 4.2, we describe

theoretical consideration and determination of parameters for the rigid ion model. Section
4.3 describes the results and discussion followed by conclusion in section 4.4.

4.2 Theoretical Consideration

The details of the theoretical model namely the Rigid ion model (RIM) used for
the calculation of phonon and allied properties at ambient and at high pressure have
already been presented in chapter (3). However, in the present section, we briefly discuss
the theoretical consideration and computational details including the optimization of the
model parameters at ambient and high pressures for the calculation of phonon properties.

The RIM of Kunc [44] provides a basis for discussing the effect of pressure on
phonon related properties, which depend on phonon frequencies only and do not require
us to consider phonon eigen vectors. The RIM parameters are two first neighbor force
constant (A and B), eight second neighbor force constants where in our case indices 1,2
represents cation and anion respectively and the effective charge parameter $Z = \dfrac{e^*}{\sqrt{\varepsilon_\infty}}$.

Two sets of RIM force constants, one at ambient and the other at high pressure are
obtained for each compound in the zinc blende III-V nitride family by using novel
optimization procedure. In estimating the $P \neq 0$, lattice constant, Muranaghan's equation
of state is adopted in relating the volume dependence to pressure. In the optimization
process of RIM parameters at ambient and high pressures, we followed the least square
fitting procedure where the data on elastic constants are used as input parameters and the
values of phonon frequencies at critical points as constraints on the values of the
parameters. To asses, the significance of the two sets of the force constants and to treat
the phonon properties at any desired pressure a linear interpolation scheme is adopted.

As far as thermodynamical properties of solids are concerned these occur in
anharmonic models when the second order coefficients in the potential energy are volume
dependent. However, to a first approximation thermal properties can be derived within
the quasi-harmonic theory by treating the lattice vibrations as harmonics, but with

assumed volume and pressure dependent phonon frequencies. In this approximation, the vibrational entropy can be expressed as the sum of the contribution from $\omega_j(\vec{q})$ phonons. The model parameters obtained by the methodology discussed above are presented in Table 2, while the input parameters used to obtain the model parameters are presented in
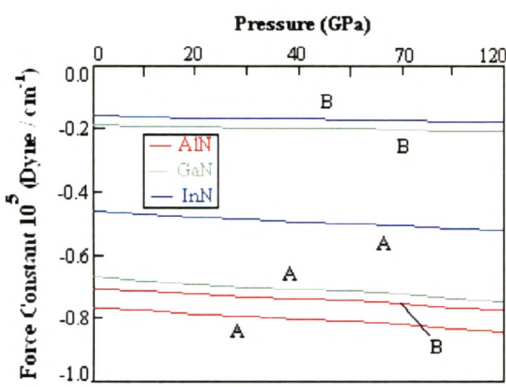
Figure 1 (a): Force constant (A and B) as a function of pressure for AlN, GaN and InN.
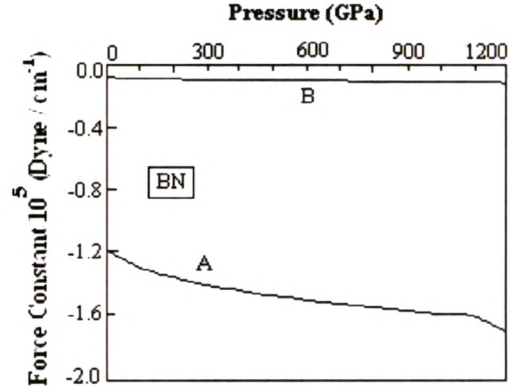
Figure 1 (b): Force constant (A and B) as a function of pressure for BN.

Table 1. An inspection of the Table 2 reveals that the trends of the variation of the force constants in these compounds seem to be physical and justified. We plot first neighbor force constant (A and B) for zinc blende AlN, GaN, InN and BN compound semiconductors in figure 1 as a function of pressure which shows the systematic variation of these parameters .

Table 1: RIM input parameters for III-Nitrides. Elastic constants C_{ij} (x 10^{11} dyne / cm^2).

Input Parameters for III-Nitrides				
Parameter	**InN**	**GaN**	**AlN**	**BN**
C_{11}	18.7	29.3	30.04	82.0
C_{12}	12.5	15.9	16.0	19.0
C_{44}	8.6	15.5	19.3	48.0
M_1 (amu)	114.82	69.72	26.98	10.81
M_2 (amu)	14.00	14.00	14.00	14.00
a (Å)	4.98	4.50	4.37	3.615
ω_{LO} (cm^{-1})	588	742	908	1285
ω_{TO} (cm^{-1})	457	553	653	1055

Table 2 (a): Calculated RIM parameters (10^5 dyne / cm) (A,B, C_i, D_i, F_i, i=1,2) for zinc blende InN. Z is a proton charge. The lattice parameter a is in Å.

RIM Parameters for InN

Parameters	0 GPa	10 GPa	20 GPa	30 GPa	40 GPa	50 GPa	70 GPa	100 GPa	120 GPa
A	-0.4600	-0.4689	-0.4763	-0.4835	-0.4941	-0.4975	-0.5041	-0.5157	-0.5204
B	-0.1572	-0.1602	-0.1627	-0.165	-0.1667	-0.1679	-0.1701	-0.174	-0.1756
C_1	-0.0504	-0.0513	-0.0521	-0.0528	-0.0537	-0.0541	-0.0548	-0.0561	-0.0566
D_1	-0.1507	-0.1536	-0.156	-0.1582	-0.1607	-0.1619	-0.164	-0.1678	-0.1693
E_1	0.0912	0.0929	0.0943	0.0956	0.0975	0.0978	0.0991	0.1014	0.1023
F_1	0.0520	0.0585	0.0658	0.074	0.0832	0.0936	0.1185	0.1631	0.2064
C_2	-0.0120	-0.0122	-0.0124	-0.0126	-0.0128	-0.0129	-0.0131	-0.0134	-0.0135
D_2	0.0250	0.0253	0.0257	0.0261	0.0264	0.0265	0.0268	0.0274	0.0276
E_2	-0.1034	-0.1054	-0.1070	-0.1085	-0.1103	-0.1111	-0.1126	-0.1152	-0.1163
F_2	-0.0205	-0.0209	-0.0213	-0.0216	-0.0219	-0.0220	-0.0223	-0.0228	-0.0230
Z	1.0500	1.0298	1.0138	0.9998	0.9836	0.9768	0.9638	0.9416	0.9329
a	4.9800	4.8838	4.8079	4.7418	4.6649	4.6325	4.5707	4.4655	4.4245

Table 2 (b): Calculated RIM parameters (10^5 dyne / cm) (A,B, C_i, D_i, F_i, i=1,2) for zinc blende GaN, Z is a proton charge. The lattice parameter a is in Å.

	RIM Parameters for GaN							
Parameters	0 GPa	10 GPa	20 GPa	30 GPa	40 GPa	50 GPa	70 GPa	100 GPa
A	-0.6651	-0.6819	-0.6914	-0.7000	-0.7067	-0.7127	-0.7234	-0.7379
B	-0.1850	-0.1881	-0.1907	-0.1932	-0.1951	-0.1968	-0.2014	-0.2054
C_1	-0.0200	-0.0203	-0.0205	-0.0207	-0.0212	-0.0214	-0.0219	-0.0223
D_1	-0.2855	-0.2900	-0.2941	-0.2977	-0.3005	-0.3031	-0.3102	-0.3164
E_1	0.0912	0.0926	0.0941	0.0952	0.0961	0.0970	0.0993	0.1013
F_1	0.0550	0.0650	0.0768	0.09079	0.1073	0.1268	0.1771	0.2500
C_2	-0.0120	-0.0122	-0.0124	-0.0126	-0.0128	-0.013	-0.0133	-0.0136
D_2	0.0625	0.0635	0.0644	0.0652	0.0658	0.0661	0.0676	0.0690
E_2	0.0034	0.0034	0.0035	0.0035	0.0035	0.0036	0.0037	0.0038
F_2	-0.0100	-0.0102	-0.0104	-0.0106	-0.0107	-0.0107	-0.011	-0.0112
Z	1.1450	1.1266	1.1111	1.0976	1.0871	1.0778	1.0529	1.03172
a	4.5000	4.4294	4.3683	4.3152	4.274	4.2377	4.1738	4.0898

Table 2 (c): Calculated RIM parameters (10^5 dyne / cm) (A,B, Ci, Di, Fi, i=1,2) for zinc blende AlN. Z is a proton charge. The lattice parameter a is in Å.

Parameters	RIM Parameters for AlN									
	0 GPa	10 GPa	20 GPa	30 GPa	40 GPa	50 GPa	60 GPa	70 GPa	100 GPa	120 GPa
A	-0.7643	-0.7722	-0.7848	-0.7932	-0.8005	-0.8065	-0.8125	-0.8179	-0.832	-0.8407
B	-0.7039	-0.7112	-0.7228	-0.7305	-0.7372	-0.7427	-0.7482	-0.7531	-0.767	-0.7738
C1	-0.0158	-0.0159	-0.0162	-0.0164	-0.0160	-0.0168	-0.0169	-0.017	-0.0173	-0.0175
D1	0.0230	0.0233	0.0236	0.0239	0.0241	0.0243	0.0245	0.0247	0.0251	0.0253
E1	0.0912	0.0921	0.0935	0.0946	0.0956	0.0963	0.0970	0.0976	0.0993	0.1003
F1	0.0100	0.0135	0.0182	0.0246	0.0332	0.0448	0.0540	0.0605	0.0923	0.1250
C2	-0.0158	-0.0159	-0.0162	-0.0164	-0.0166	-0.0168	-0.0169	-0.017	-0.0173	-0.0175
D2	-0.0215	-0.0217	-0.0220	-0.0222	-0.0224	-0.0226	-0.0228	-0.023	-0.0234	-0.0236
E2	0.1034	0.1045	0.1063	0.1075	0.1085	0.1093	0.1011	0.1018	0.1134	0.114
F2	0.0005	0.0005	0.0005	0.0005	0.0005	0.0005	0.0005	0.0005	0.0005	0.0005
Z	1.2500	1.2371	1.2169	1.204	1.1929	1.1841	1.1753	1.1675	1.1437	1.1331
A	4.3700	4.3248	4.2545	4.2094	4.1708	4.1398	4.1089	4.0817	4.007	3.9698

Table 2 (d): Calculated RIM parameters (10^5 dyne / cm) (A,B, Ci, Di, Fi, i=1,2) for zinc blende BN.Z is a proton charge. The lattice parameter a is in Å.

	RIM Parameters for BN												
Parameters	0 GPa	100 GPa	200 GPa	300 GPa	400 GPa	500 GPa	600 GPa	700 GPa	800 GPa	900 GPa	1000 GPa	1100 GPa	1200 GPa
A	-1.175	-1.2852	-1.3481	-1.3945	-1.4319	-1.4634	-1.4908	-1.5154	-1.5374	-1.5577	-1.5762	-1.5934	-1.6936
B	-0.0812	-0.0888	-0.0931	-0.0963	-0.0989	-0.1011	-0.1030	-0.1047	-0.1062	-0.1076	-0.1089	-0.1101	-0.1170
C1	-0.2008	-0.2196	-0.2303	-0.2383	-0.2447	-0.2500	-0.2547	-0.2589	-0.2627	-0.2662	-0.2693	-0.2723	-0.2894
D1	0.1556	0.1702	0.1785	0.1846	0.1896	0.1937	0.1974	0.2006	0.2036	0.2062	0.2087	0.2110	0.2242
E1	0.0912	0.0997	0.1046	0.1082	0.1114	0.1135	0.1157	0.1176	0.1193	0.1209	0.1223	0.1236	0.1314
F1	0.0508	0.1905	0.3000	0.4000	0.5000	0.6000	0.7000	0.8000	0.8200	0.8400	0.8600	0.8800	0.9000
C2	-0.0888	-0.0971	-0.1018	-0.1053	-0.1082	-0.1106	-0.1126	-0.1145	-0.1161	-0.1177	-0.1191	-0.1204	-0.1280
D2	-0.0556	-0.0608	-0.0637	-0.0659	-0.0677	-0.0692	-0.0705	-0.0717	-0.0727	-0.0737	-0.0745	-0.0754	-0.0801
E2	0.0034	0.0037	0.0039	0.0040	0.0041	0.0042	0.0043	0.0043	0.0044	0.0045	0.0045	0.0046	0.0049
F2	-0.0305	-0.0333	-0.0350	-0.0362	-0.0371	-0.0379	-0.0387	-0.0393	-0.0399	-0.0404	-0.4091	-0.0413	-0.0439
Z	0.9500	0.8608	0.8187	0.7905	0.7693	0.7524	0.7383	0.7261	0.7155	0.7061	0.6977	0.6901	0.0646
a	3.6150	3.2757	3.1154	3.0082	2.9276	2.8632	2.8095	2.7632	2.7230	2.6872	2.6552	2.6261	2.4611

4.3 Results and Discussion

4.3.1 Phonon Dispersion Curves

For systematic study of the phonon properties of III-V nitrides semiconductors under pressure, we have calculated the complete phonon dispersion curves at different pressure close to the phase transition pressure by using the rigid ion model discussed in previous chapter and parameters obtained in section 2. The pressure dependent phonon dispersion curves have been carried out for some selected semiconductors namely AlN, GaN, InN and BN. The results thus obtained are discussed below.

The phonon dispersion curves for InN, GaN, AlN and BN at ambient and at high pressure have been presented in figure. (2) along high symmetry directions$(\vec{q},0,0)$, $(\vec{q},\vec{q},0)$ and$(\vec{q},\vec{q},\vec{q})$. We only plot the high pressure phonon dispersion curves for one value close to the phase transition pressure. The phase transition pressure for BN is > 1100 GPa [45 - 46], AlN is in the range of 20 GPa [47-48] and for GaN it is the range of 60 GPa [49-51]. However, the investigation has been performed for several other high pressure cases but not presented here. The results have been compared with the available data [52-56].
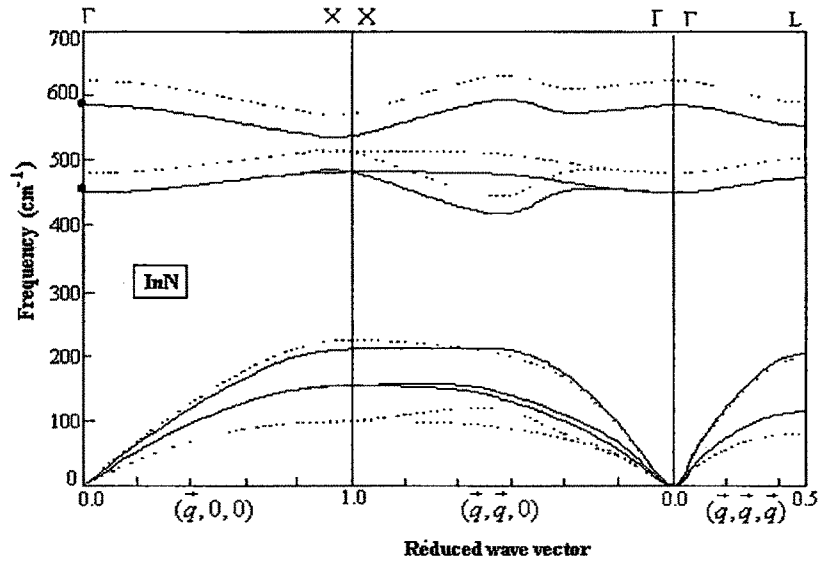
Figure 2 (a): RIM calculations of the phonon dispersion for zinc blende InN semiconductor. Solid and dotted lines represents ambient and 100 GPa calculations. Filled circles represent experimental values [56].
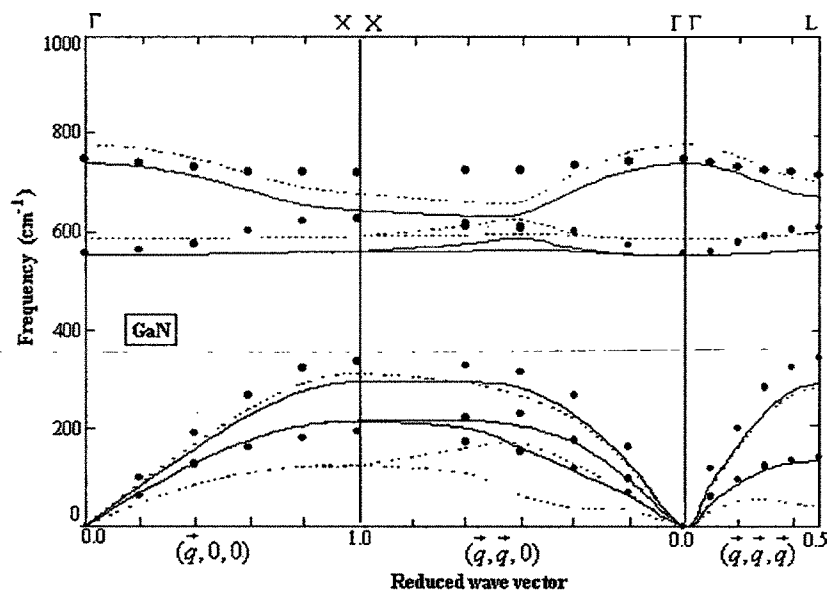
Figure2 (b): RIM calculations of the phonon dispersion for zinc blende GaN semiconductor. Solid and dotted lines represent ambient and 100 GPa calculations. Filled circles represent experimental values [52-56].
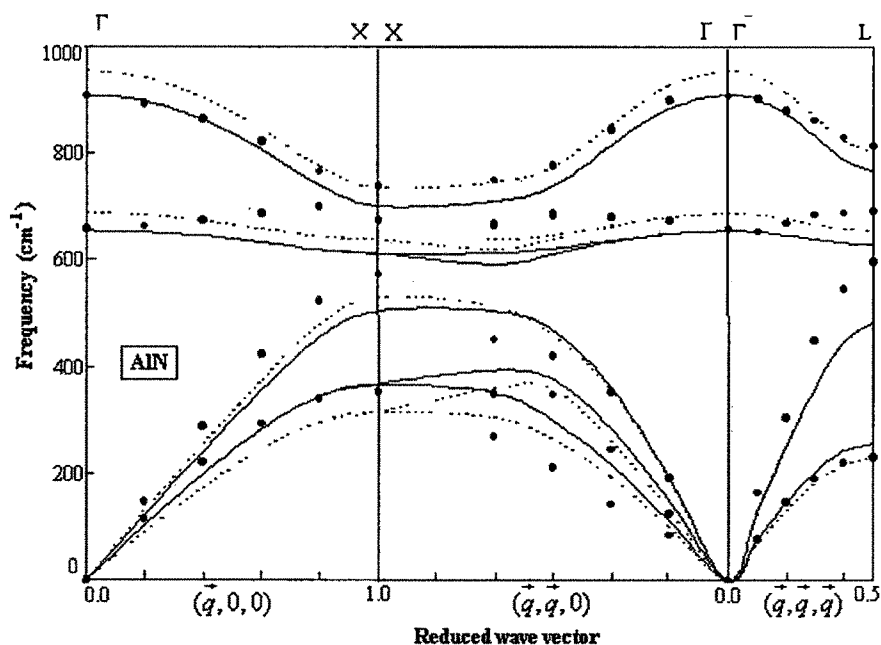
Figure 2 (c): RIM calculations of the phonon dispersion for zinc blende AlN semiconductor. Solid and dotted lines represent ambient and 120 GPa calculations. Filled circles represent experimental values [52-56].
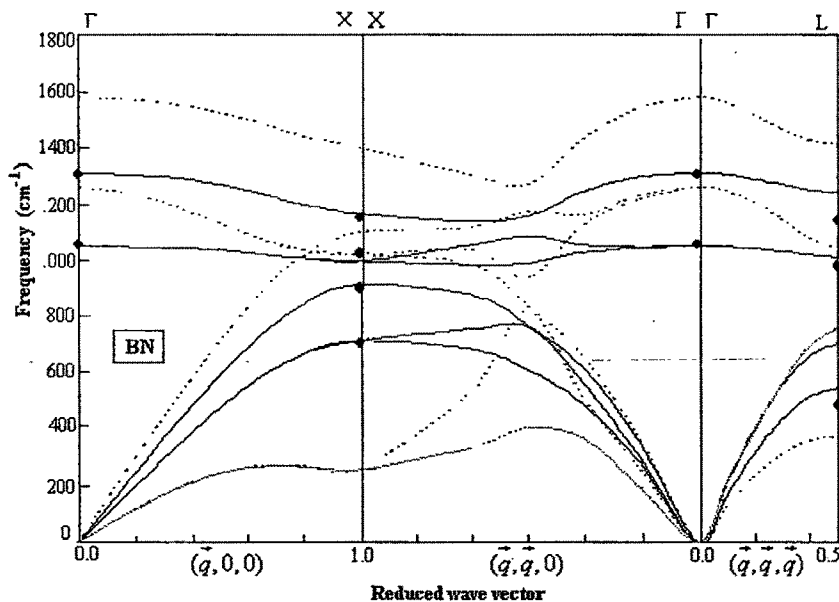
Figure 2 (d): RIM calculations of the phonon dispersion for zinc blende BN semiconductor. Solid and dotted lines represent ambient and 100 GPa calculations. Filled circles represent experimental values [56].

The values of critical point phonons at ambient pressure are found in good agreement with the existing experimental data. As these figures reveal, while the optical branch is more or less dispersive particularly in $(\vec{q},0,0)$ and $(\vec{q},\vec{q},0)$ directions of the Brillouin Zone (BZ), the acoustic phonon modes are almost flat at X and L point of Brillouin Zone with usual increasing frequencies going from low to higher wave vectors. As far as the effect of pressure on the phonon dispersion is concerned the nature of phonon band structure is more or less similar to the ambient pressure except TA branch. However, the quantitative analysis reflects an increase in LO, TO and LA phonon frequencies with pressure and decrease in TA phonon mode frequencies through out the Brillouin Zone (BZ). To have an idea, these frequencies at different critical points of the BZ have been plotted with pressure for all four considered nitrides in figure 3-6. Here we summarize some of the silent features found in the phonon behavior.
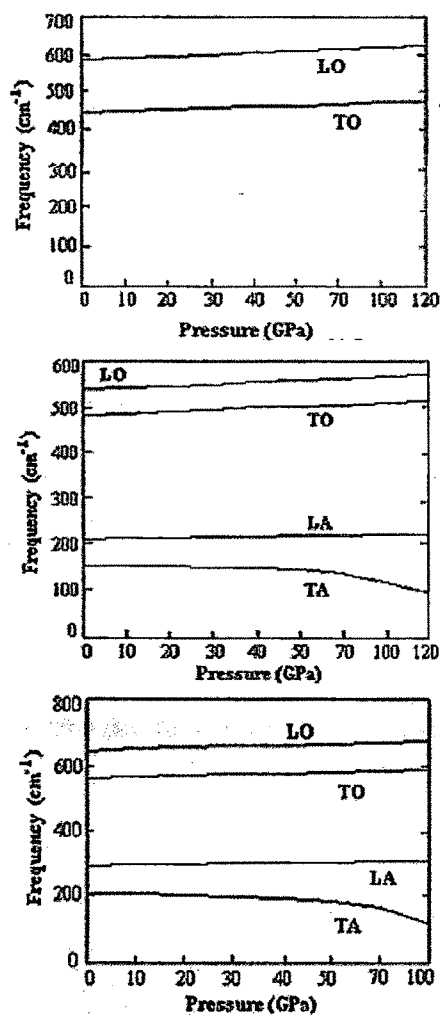
Figure 3: Variation of (a) ω_{LO}, ω_{TO} at Γ -point (b)ω_{LO}, ω_{TO}, ω_{LA} and ω_{TA} at X , and (c) ω_{LO}, ω_{TO}, ω_{LA} and ω_{TA} at L with pressure for InN.
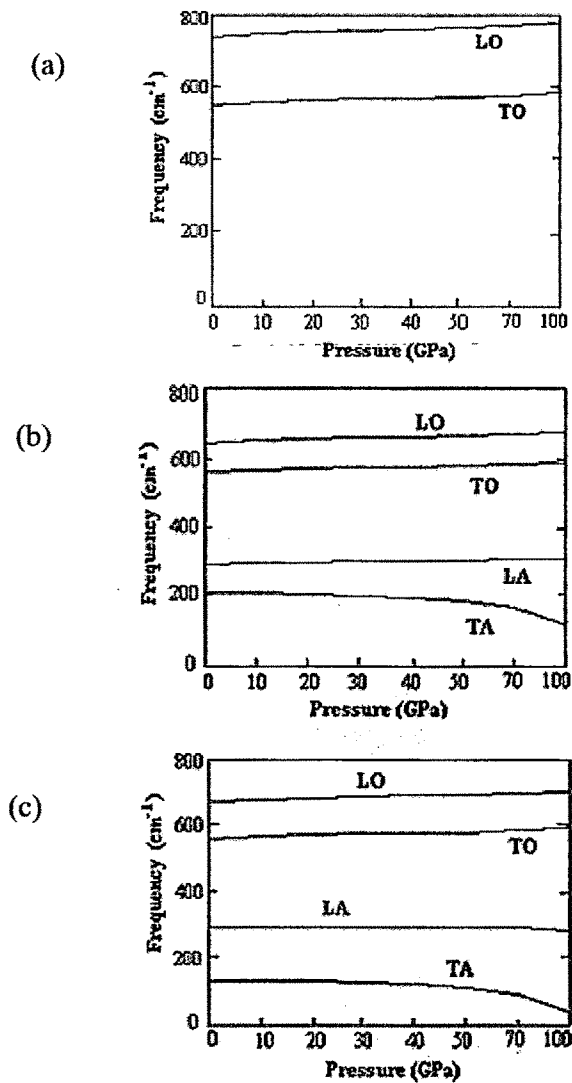
Figure 4: Variation of (a) ω_{LO}, ω_{TO} at Γ -point (b)ω_{LO}, ω_{TO}, ω_{LA} and ω_{TA} at X , and (c) ω_{LO}, ω_{TO}, ω_{LA} and ω_{TA} at L with pressure for GaN.
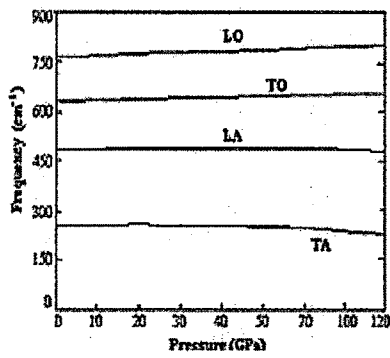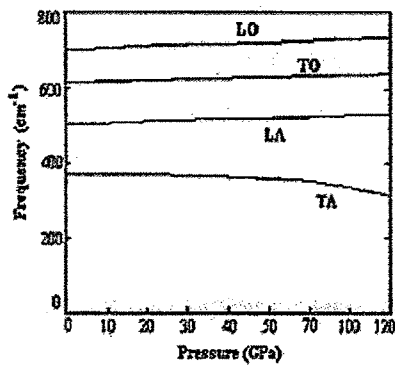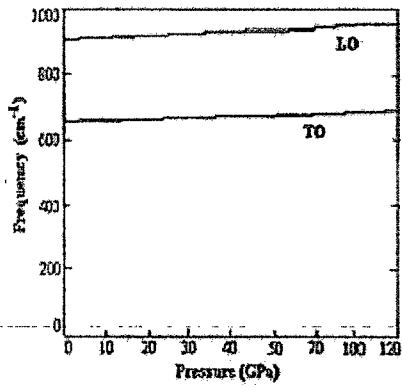
Figure 5: Variation of (a) ω_{LO}, ω_{TO} at Γ -point (b) ω_{LO}, ω_{TO}, ω_{LA} and ω_{TA} at X and (c) ω_{LO}, ω_{TO}, ω_{LA} and ω_{TA} at L with pressure for AlN.
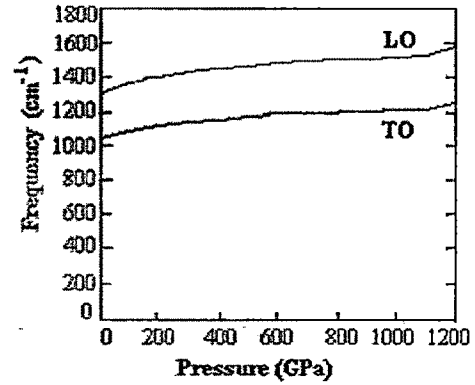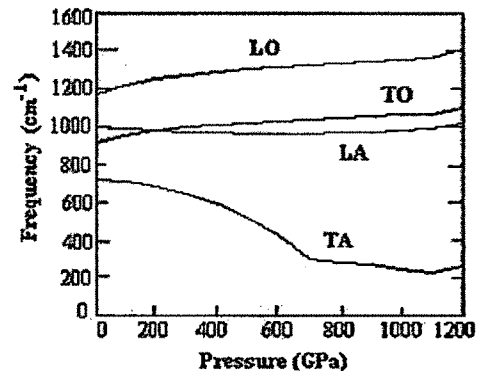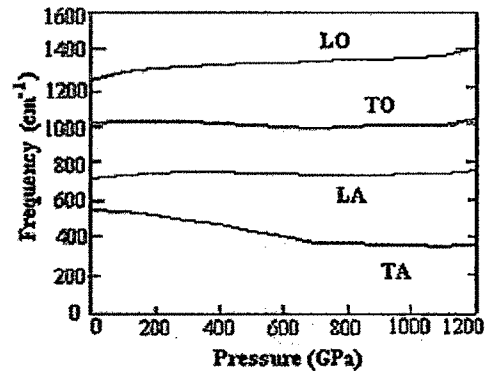
Figure 6: Variation of (a) ω_{LO}, ω_{TO} at Γ -point (b) ω_{LO}, ω_{TO}, ω_{LA} and ω_{TA} at X , and (c) ω_{LO}, ω_{TO}, ω_{LA} and ω_{TA} at L with pressure for BN.

❖   For the InN→ GaN→ AIN→ BN sequence where N atom is common, the zone center optical phonon modes increases with the decrease with the cation mass. Similarly, the phonon gap between two optical- acoustic bands decreases with increase in the anion to cation mass ratio.

❖   In III- nitrides, the strength of elastic forces and the degree of mixture of ionic and covalent bonding are responsible for the LO-TO splitting at zone center as well as for the distinct behavior of the optical and acoustical phonon. As compared to BN and AIN when the LO phonons show pronounced dispersive behavior, in GaN and InN the dispersion of LO mode is shallower. The TO branches in BN and AIN show no or very little dispersion whereas upward dispersion is revealed for the TO phonons in GaN and InN. The figure (7) presents the pressure dependent LO-TO splitting at zone center for InN, GaN, AIN and BN respectively.
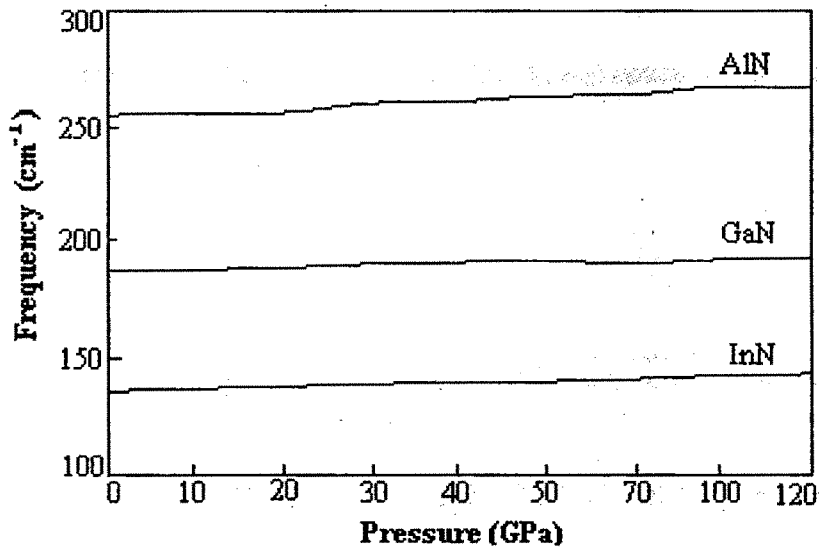
Figure 7 (a): Pressure variation for $\omega LO - \omega_{TO}$ at Γ- point for InN, GaN and AIN.

It is seen from these figures that the LO-TO splitting shows linear increase with the pressure which is maximum for BN. This indicates that pressure affects the ionicity of the compounds. This is due to the fact that under pressure the change in splitting of the optical phonon frequencies at the zone center point may cause a

redistribution of the Szigetti's effective charge on the ions that in turn affect the ionicity of semiconductors.
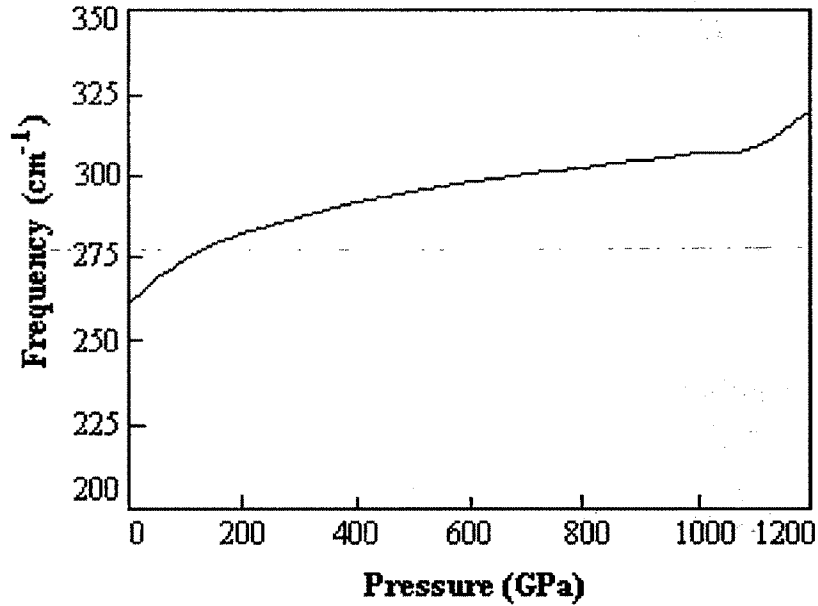
Figure 7 (b): Pressure variation for $\omega LO - \omega TO$ at Γ- point for BN.

❖   Similar to III-V compounds, Our calculation shows flatness of the TA branches over part of the BZ in GaN and InN. In AlN and BN, however this features disappears either partially or completely.

4.3.2   Phonon Density of States

Besides phonon dispersion curves, we have also calculated the phonon density of states for InN, GaN AlN and BN. The phonon density of states presents an over all view of the range and extent of various phonon modes in the lattice. The calculation of one phonon density of states is vital as it requires the determination of phonon modes in whole BZ. One phonon density of states at different pressures for these compounds calculated by using methodology discussed in chapter 3 have been displayed in Figure (8). These figures show that frequency spectrum shifts towards higher frequency as the pressure is increased. The height of the peaks, however decrease with an increase in pressure. As far as the common features at ambient and high pressure for these

compounds are concern it can be seen from the present figures that our results exhibits a gradual development of the sharp density of states with distinct LO and TO phonons, as one moves from InN $\rightarrow$ GaN$\rightarrow$ AlN $\rightarrow$ BN. It is also seen sharp and
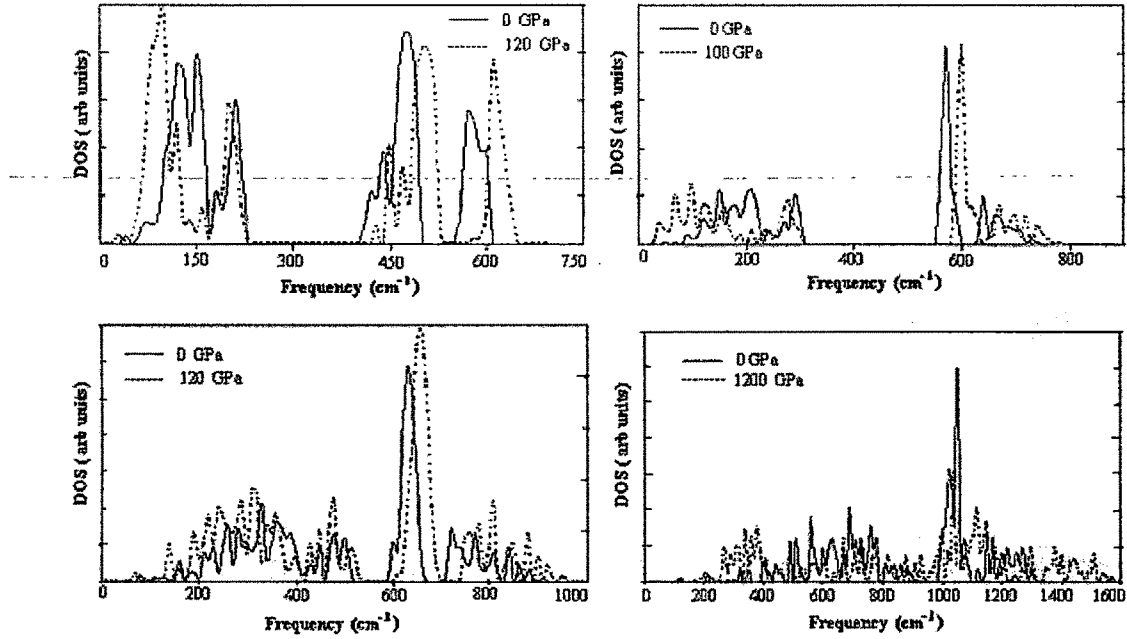
Figure 8: One phonon density of states for InN, GaN, AlN and BN.

Pronounced peaks in the TA region of the one phonon density of states while broad band appears in the corresponding region of AlN and BN. The pressure causes the shift of phonon peaks in all four nitrides. While the peaks associated with transverse acoustic phonon mode shifts towards lower side, the peaks in the high frequency sides shifts towards higher frequency side of the spectrum. These figures also reveal the appearance of the new peaks in both sides of the spectra. Very intense peak in the middle of the spectra is basically due to the contributions of LA and TO phonon modes throughout the Brillouin zone.

4.3.3 Mode Grüneisen Parameter

In describing the volume or pressure dependence of the phonon frequencies in solids, Barron [57] has introduced the mode Grüneisen parameter γ_i , which has been
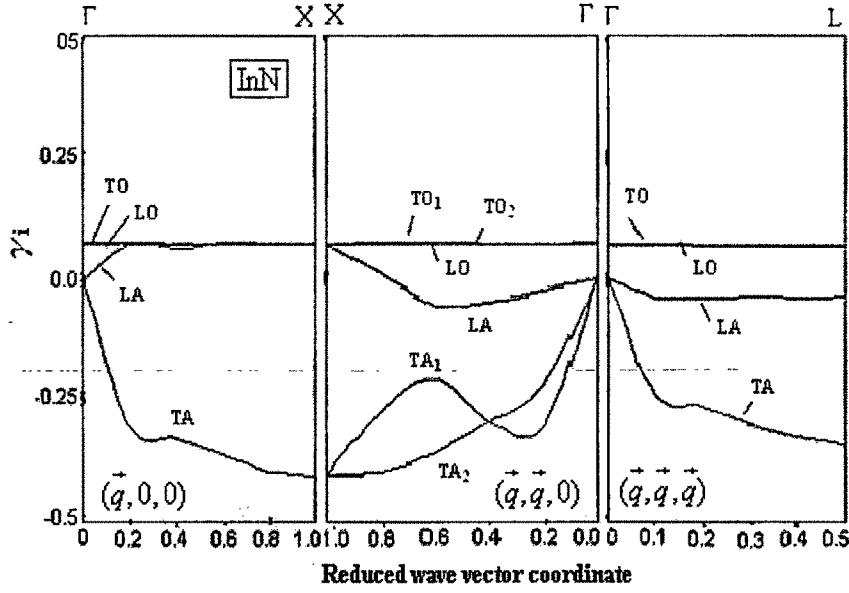
Figure 9(a): Calculated mode Grüneisen parameter along high symmetry directions for InN.
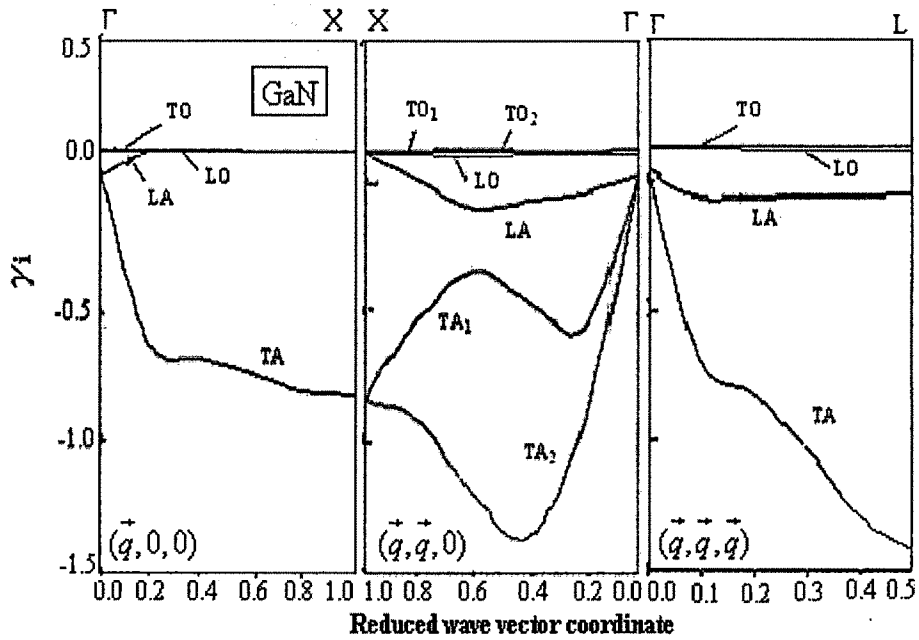
Figure 9 (b): Calculated mode Grüneisen parameter along high symmetry directions for GaN.

80
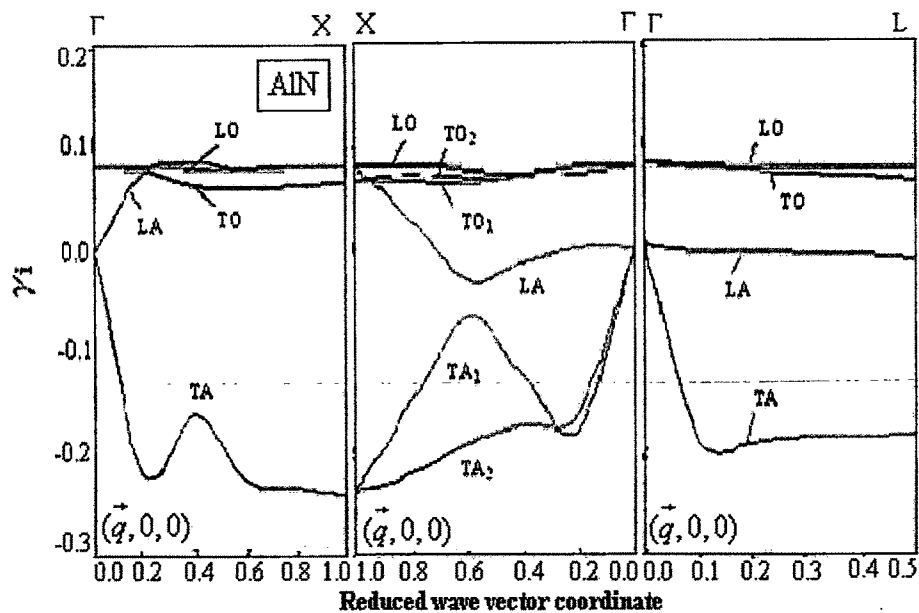
Figure 9 (c): Calculated mode Grüneisen parameter along high symmetry directions for AlN.
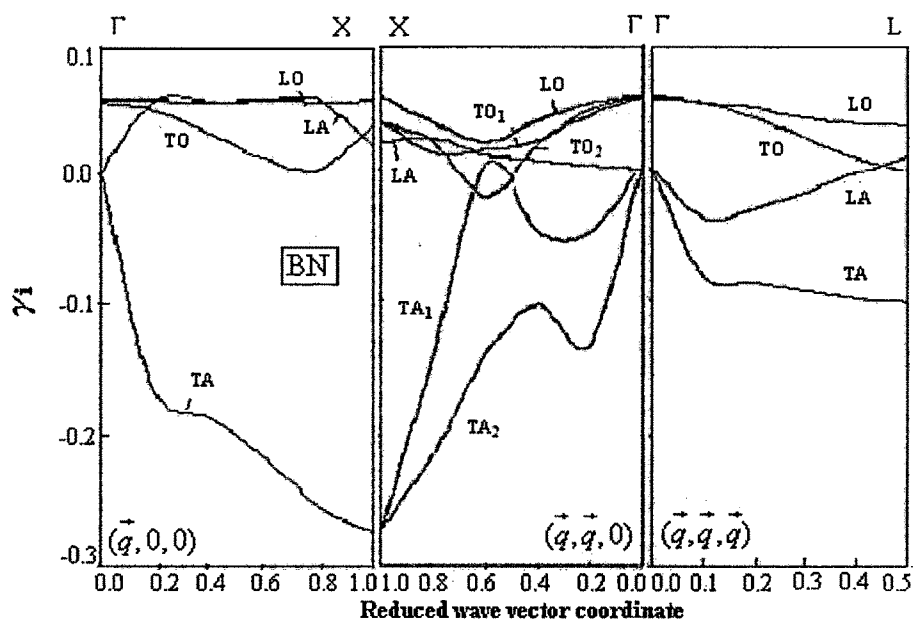
Figure 9 (d) Calculated mode Grüneisen parameter along high symmetry directions for BN.

described in chapter 3. The knowledge of mode Grüneisen parameter are known in a solid for all branches through out the BZ, the responsible phonon mode or modes can be found along with the determination of thermal expansion. The calculated values of the $\omega_i(\bar{q})$ and $\dfrac{d\omega_i(\bar{q})}{dP}$ as a function of wave vector $\bar{q}$ through out the Brillouin Zone are used to study the variation of the mode Grüneisen parameter $\gamma_i(\bar{q})$. The results along $(\bar{q},0,0),(\bar{q},\bar{q},0)$ and $(\bar{q},\bar{q},\bar{q})$ for all four III-V nitrides are displayed in figure (9). These figures reveal that mode Grüneisen parameters for the TA branches in III- nitrides are negative while for all other branches they are almost positive, but with very small value. This may be due to the compensation between central and non central forces in cubic III-nitrides. Also this indicates that the lattice softening of the TA phonons is primarily responsible for the observed phase transition in these compounds.

4.3.4 Lattice Specific heat at Constant Volume

Table 3: Specific heat (Joule/ mole-K) for AlN, GaN, InN, and BN with pressure.

Pressure	AlN	GaN	InN	Pressure	BN
0 GPa	39.24	109.51	164.61	0 GPa	5.60
20 GPa	38.80	111.00	165.00	100 GPa	5.78
				200 GPa	6.20
40 GPa	39.40	122.55	168.12	400 GPa	7.71
70 GPa	41.02	140.14	175.27	640 GPa	11.46
100 GPa	43.76	185.24	190.43	800 GPa	17.00
				1000 GPa	18.77
120 GPa	47.57	-----	212.18	1200 GPa	16.81

The lattice specific heat constant volume is a quantity, which basically tests the success of model calculations. We have calculated the pressure dependent lattice specific heat at constant volume C_v at room temperature by using the expression presented in chapter 3, and presented in Table (3). The Table (3) reveals that the C_v increases with pressure for all considered III-nitrides and values obtained at ambient condition are in good agreement. As far as the increase of C_v with pressure is concerned it is quite

obvious due to the modifications of phonon spectra particularly acoustic phonon branches.

4.4 Conclusions

A comprehensive study for the pressure induced vibrational properties of III-nitrides is reported using a realistic dynamical model. In this macroscopic approach, once the pressure dependence of the model parameters in a solid is accurately established, nearly all of its vibrational properties at $P \neq 0$ can be predicated with reasonable success. In conclusion, we have calculated the pressure dependence of the phonon dispersion curves, phonon density of states, mode Grüneisen parameters, and specific heat at constant volume for III- nitrides namely InN, GaN, AlN and BN by using rigid ion model. It is observed that the energies of the optical phonons (both longitudinal and transverse) as well as longitudinal acoustic phonons while the transverse acoustic phonon energy decrease increase with pressure. Phonon density of states calculated at high pressure of corresponding solid, show pronounced shift in the frequency spectra with pressure. The mode Grüneisen parameter indicates that the TA phonon modes have negative values and responsible for the lattice softening. Specific heat at constant volume, C_v increases with pressure for all compounds.

References

1. *Diluted Magnetic Semiconductors,* edited by R L Aggrawal, J K Furdyana and M S Von, **89**, (Mat. Research Society Symposia Proceedings, Pitsburg, 1987).

2. R R Galazka, *Proc. 14th international conference on the physics of semiconductors,* Edinburgh, edited by B L H. Wilson (Inst. of Phys.), 133, 1978.

3. J K Furdyana, *J.of appl. Phys.* **64**, R 29 (1988).

4. *Semiconductors and semimetals,* edited by R K Willardon, A C Beer and J K Furdyana (Academic Press Boston) **25**, (1998).

5. N Samarth and J K Furdyana, *Proc. IEEE,* **78**, 990 (1990).

6. *Diluted Magnetic Semiconductors,* edited by Mukesh Jain (World Scientific, ingapore), 1991.

7. A V Kamarov, S M Pjabchenko, O V Terletski, I I Zhem and R D Ivanchuk, *J.of Appl. Phys.* **73**, 608 (1977).

8. F Herman, *J. Appl. Chem. Solids* **8**, 405 (1959).

9. V Yu Davydov, Yu.B Kitaev, L N Gonchark and A N Smirnov, *Phys. Rev.* **B58**, 12899 (1999).

10. T D Moustakas, L Lei and R J Molnar, *Physica B* **185** 36 (1993).

11. A K Rajgopal and R Srinivasan, *J. Phys.* **158**, 471 (1960).

12. J K Vetelino and S S Mitra, *Solid State Commun.* **7**, 1181 (1969), *Phys. Rev.* **178**, 1349 (1969).

13. R Banerjee and Y P Varshni, *J. of Phys. Soc.* (Japan) **30**, 1015 (1971).

14. A D Zdetsis, *Phys Rev. Lett.* **60**, 63 (1977).

15. A D Zdetsis and C S Wang *Phys Rev.* **19**, 2999 (1979).

16. B G Dick and AW Overhauser, *Phys Rev.* **B112**, 90 (1958).

17. H Bliz, *Computational Solid State Physics* (Plenum press, New York, 1972).

18. J R Hardy, *Philos. Mag.* **7**, 315 (1962).

19. K Kunc, M Balkanski and M Nusimovici, *Phys.* State Solidi (b) **72**, 229, (1975).

20. M S Kushwaha, *J.Chem. Phys.* **81**, 2028 (1984).

21. S S Jaswal, *Lattice Dynamics,* ed. M Balkanski, 41 (Flammarion Press, Paris 1977).

22. G Dolling and J L T Waugh, *Lattice Dynamics,* ed. R F Wallis, 19 (Pergamon Press, Oxford, 1965).

23. J L Yarnell, J L Waerren and R G Wenzel, *Neutron Inelastic Scattering* **1**, 3019 (1969) (International Atomic Agency, Veinna).

24. J A Onton, *Proc. 10th Int. Conf. Physics of Semiconductors,* Cambridge (MA) eds., S P Keller, J C Hensel and F Stern, (U. S. AEC, Springfield (VA) 1970).

25. J F Vetelino and S S Mitra, *Phys. Rev.* **178**, 1349 (1969).

26. V S Mashkewitch and K B Tolpygo, *Sov. Phys.* JETP **5**, 435 (1957).

27. H L Mcmurry, A W Volbrig, J K Boytter and C Noble, *J. Phys Chem.* **28** 2359 (1967).

28. J L Yarnell, J L Warren, R G Venzel and P J Dean, In the fourth IAEA Symposium on Inelastic Neutron Scattering (IAEA, Vienna, 1968) Vol-1, 301.

29. S J Duclos, Y K Vohra and A L Ruoff, *Phys. Rev. Lett.* **58**, 775 (1987).

30. O Brafman, M Cardona and Z Verdeng, *Phys. Rev.* **B15**, 1081 (1977).

31. B A Weinstein, *Solid State Commun.* **24**, 595 (1975).

32. B A Weinstein and R Zallen, in *Light Scattering Solids,* Vol. **IV** in Springer Series topics in Applied Physics, edited by M. Cardona and G. Guntherodt (Springer-Verlag, Berlin 1984).

33. R Trommer, E Anastassakis and M Cardona, in *Light Scattering Solids,* edited by M Balkanski, R C C Leite, and S P S Porto (Flammarion, Paris, 1976) 396.

34. R. Trommer, H. Muller, M. Cardona and P. Vogl, *Phys. Rev.* **B21**, 4869 (1980).

35. B A Weinstein, J B Renucci and M Cardona, *Solid State Commun.* **12**, 473 (1973).

36. T Soma, J Satoh and H Matsuo, *Solid State Commun.* **42**, 889 (1982), T Soma and K Kudo *J. Phys. Soc. Jpn.* **48**, 115 (1980).

37. C Patel, W F Sherman and G R Wilkinson, *J. Mol. Struct.* **79**, 297 (1982).

38. S Froyen and M L Kohen, *Solid State Commun.* **43**, 447 (1982).

39. K Karch and F Bechstedt, *Phys. Rev.* **B56**, 7404 (1997).

40. C Gobel, C Schrepet, U Schrez, P Thurian, G Kaczmarezyk and A Hofmann, *Mat. Sci. forum* **25** 11173 (1997).

41. K Miwa and A Fukumato, *Phys. Rev.* **B48**, 7879 (1993).

42. K Kim, W R L Lambrecht and B Segall, *Phys. Rev.* **B50**, 1502 (1994).

43. P Perlin, A Polian and T Suski, *Phys. Rev.* **B47**, 2874 (1993).

44. K Kunc and O Holm Nielsen, *Computer physics Communications* 16, 81 (1979).

45. R M Wentzcovitch, K J Chang and M L Cohen, *Phys. Rev.* **B34**, 1071 (1986).

46. R M Wentzcovitch. M L Cohen and P K Lam, *Phys. Rev.* **B36**, 6058 (1987).

47. P E Van Camp, V E Van Doren and J T Devreese, *Phys. Rev.* **B44**, 9056 (1991).

48. I Gorczyca, N E Christensen, P Perlin, I Grzegory, J Jun and M Bockwoski, *Solid State Commun.* **79**, 1033 (1991).

49. A Munoz, K Kunc, *Phys. Rev.* **B44**, 10372 (1991).

50. I Gorezyca and N E Christensen, *Solid State Commun.* **80**, 335 (1991).

51. P E Van Camp, V E Van Doren and J T Devereese, *Solid State Commun.* **81**, 23 (1992).

52. P Perlin, C Jauberthie-Carillon, J P Itie, A San Miguel, I Grzegory, and A Polian, *Phys. Rev.* **B45**, 83(1992);P Perlin, T Suski, J W Ager III, G Conti, A Polian, N E Christensen, I Gorczyca, I Grzegory, E R Weber and E E Haller, *Phys. Rev.* **B60**, 1480 (1999).

53. H Siegle, A R Goñi, C Thomsen, C Ulrich, K Syassen, B Schöttker, D J As, and D Schikora, in: *Gallium Nitride and Related Materials* II, Eds. by C R Abernathy H Amano, and J C Zopler, *Mater. Res. Soc. Symp. Proc.* **468** (Material Research Society, Pittsburgh, 1997), p. 225.

54. A R Goñi, H Siegle, K Syassen, C Thomsen, and cJ M Wagner, *Phys. Rev.* **B64**, 035205-1 (2001).

55. Z X Liu, A R Goñi, K Syassen, H Siegle, C Thomsen, B Schöttker, D J As, and D Schikora, *J. Appl.Phys.* **86**, 929 (1999).

56. U Grossner, J Furthmuller and F Bechstedt, Proc. Int. workshop on Nitride Semiconductor, IPAP Conf. Series-I, 56-59.

57. T H K Baron, *Ann. Phys.* (N.Y.) **1**, 77 (1957).